

Supplementary tables

Supplementary table 1. Comparison of FcγRI-binding profiles by BGB-A317 and BGB-A317/IgG4_{S228P}

	k_a (1/Ms)	k_d (1/s)	K_A (1/M)	K_D (M)
BGB-A317/IgG4 _{S228P}	7.12×10^5	1.99×10^{-3}	3.57×10^8	2.80×10^{-9}
BGB-A317	ND	ND	ND	ND

K_A : affinity. K_D : dissociation constant. ND: not detectable.

Supplementary table 2. Comparison of PK parameters between BGB-A317 and BGB-A317/IgG4_{S228P}

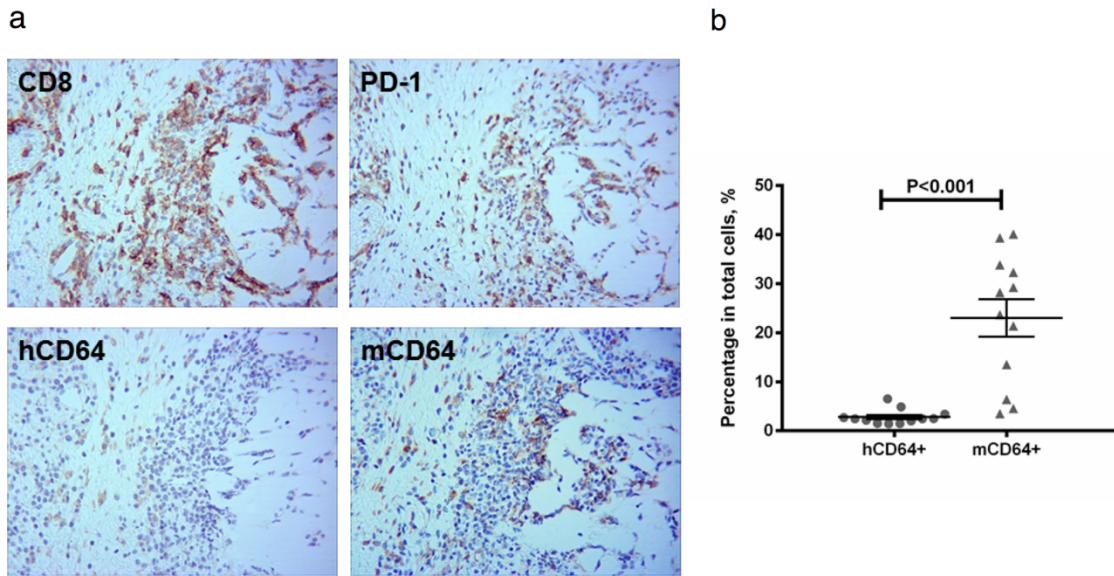
	Dose (mg/kg, QW)	C_{max} (μg/ml)	AUC_{0-168h} (μg/ml-h)
BGB-A317	1	10.6	1087
BGB-A317	10	112.8	11396
BGB-A317/IgG4 _{S228P}	10	73.0	6000

Supplementary figure 1

	1	11	21	31	41	51	61	71	81																																																																																	
IgG4 S228P	A	S	T	A	L	G	C	L	V	K	D	Y	F	P	E	P	V	T	V	S	W	M	S	G	A	L	T	S	G	V	H	T	F	P	A	V	L	Q	S	S	G	L	Y	S	L	S	S	V	V	T	V	P	S	S	S	L	G	T	K	T	Y	T	C	N	V	D	H	K	P	S																				
IgG4 Wt	A	S	T	A	L	G	C	L	V	K	D	Y	F	P	E	P	V	T	V	S	W	M	S	G	A	L	T	S	G	V	H	T	F	P	A	V	L	Q	S	S	G	L	Y	S	L	S	S	V	V	T	V	P	S	S	S	L	G	T	K	T	Y	T	C	N	V	D	H	K	P	S																				
BGB-A317	A	S	T	A	L	G	C	L	V	K	D	Y	F	P	E	P	V	T	V	S	W	M	S	G	A	L	T	S	G	V	H	T	F	P	A	V	L	Q	S	S	G	L	Y	S	L	S	S	V	V	T	V	P	S	S	S	L	G	T	K	T	Y	T	C	N	V	D	H	K	P	S																				
Consensus	a	s	t	a	l	g	c	l	v	k	d	y	f	p	e	p	v	t	v	s	w	m	s	g	a	l	t	s	g	v	h	t	f	p	a	v	l	q	s	s	g	l	y	s	l	s	s	v	v	t	v	p	s	s	s	l	g	t	k	t	y	t	c	n	v	d	h	k	p	s																				
	91	101	111	121	131	141	151	161	171																																																																																	
IgG4 S228P	N	T	K	V	D	K	R	V	E	S	K	Y	G	P	P	C	P	C	P	A	P	E	F	L	G	G	P	S	V	F	L	F	P	P	K	P	K	D	T	L	M	I	S	R	T	P	E	V	T	C	V	V	V	D	V	S	Q	E	D	P	E	V	Q	F	N	W	Y	V	D	G	V	E	V	H	N	A	K	T	K	P	R	E	E	Q	F	N	S	T	Y	
IgG4 Wt	N	T	K	V	D	K	R	V	E	S	K	Y	G	P	P	C	P	S	C	P	A	P	E	F	L	G	G	P	S	V	F	L	F	P	P	K	P	K	D	T	L	M	I	S	R	T	P	E	V	T	C	V	V	V	D	V	S	Q	E	D	P	E	V	Q	F	N	W	Y	V	D	G	V	E	V	H	N	A	K	T	K	P	R	E	E	Q	F	N	S	T	Y
BGB-A317	N	T	K	V	D	K	R	V	E	S	K	Y	G	P	P	C	P	C	P	A	P	V	A	G	G	P	S	V	F	L	F	P	P	K	P	K	D	T	L	M	I	S	R	T	P	E	V	T	C	V	V	V	A	V	S	Q	E	D	P	E	V	Q	F	N	W	Y	V	D	G	V	E	V	H	N	A	K	T	K	P	R	E	E	Q	F	N	S	T	Y		
Consensus	n	t	k	v	d	k	r	v	e	s	k	y	g	p	p	c	p	c	p	a	p	v	a	g	g	p	s	v	f	l	f	p	p	k	p	k	d	t	l	m	i	s	r	t	p	e	v	t	c	v	v	v	d	v	s	q	e	d	p	e	v	q	f	n	w	y	v	d	g	v	e	v	h	n	a	k	t	k	p	r	e	e	q	f	n	s	t	y		
	181	191	201	211	221	231	241	251	261																																																																																	
IgG4 S228P	R	V	V	S	V	L	T	V	H	Q	D	W	L	N	G	K	E	Y	K	C	K	V	S	N	K	G	L	P	S	S	I	E	K	T	I	S	K	A	K	G	Q	P	R	E	P	Q	V	Y	T	L	P	P	S	Q	E	E	M	T	K	N	Q	V	S	L	T	C	L	V	K	G	F	Y	P	S	D	I	A	V	E	W	E	S	N	G	Q	P	E	N	N	
IgG4 Wt	R	V	V	S	V	L	T	V	H	Q	D	W	L	N	G	K	E	Y	K	C	K	V	S	N	K	G	L	P	S	S	I	E	K	T	I	S	K	A	K	G	Q	P	R	E	P	Q	V	Y	T	L	P	P	S	Q	E	E	M	T	K	N	Q	V	S	L	T	C	L	V	K	G	F	Y	P	S	D	I	A	V	E	W	E	S	N	G	Q	P	E	N	N	
BGB-A317	R	V	V	S	V	L	T	V	H	Q	D	W	L	N	G	K	E	Y	K	C	K	V	S	N	K	G	L	P	S	S	I	E	K	T	I	S	K	A	K	G	Q	P	R	E	P	Q	V	Y	T	L	P	P	S	Q	E	E	M	T	K	N	Q	V	S	L	T	C	L	V	K	G	F	Y	P	S	D	I	A	V	E	W	E	S	N	G	Q	P	E	N	N	
Consensus	r	v	v	s	v	l	t	v	h	q	d	w	l	n	g	k	e	y	k	c	k	v	s	n	k	g	l	p	s	s	i	e	k	t	i	s	k	a	k	g	q	p	r	e	p	q	v	y	t	l	p	p	s	q	e	e	m	t	k	n	q	v	s	l	t	c	l	v	k	g	f	y	p	s	d	i	a	v	e	w	e	s	n	g	q	p	e	n	n	
	271	281	291	301	311	321	331	341	351																																																																																	
IgG4 S228P	Y	K	T	P	P	V	L	D	S	D	G	S	F	F	L	Y	S	R	L	T	V	D	K	S	R	W	Q	E	G	N	V	F	S	C	S	V	M	H	E	A	L	H	N	H	Y	T	Q	K	S	L	S	L	S	L	G	K																																		
IgG4 Wt	Y	K	T	P	P	V	L	D	S	D	G	S	F	F	L	Y	S	R	L	T	V	D	K	S	R	W	Q	E	G	N	V	F	S	C	S	V	M	H	E	A	L	H	N	H	Y	T	Q	K	S	L	S	L	S	L	G	K																																		
BGB-A317	Y	K	T	P	P	V	L	D	S	D	G	S	F	F	L	Y	S	R	L	T	V	D	K	S	R	W	Q	E	G	N	V	F	S	C	S	V	M	H	E	A	L	H	N	H	Y	T	Q	K	S	L	S	L	S	L	G	K																																		
Consensus	y	k	t	p	p	v	l	d	s	d	g	s	f	f	l	y	s	r	l	t	v	d	k	s	r	w	q	e	g	n	v	f	s	c	s	v	m	h	e	a	l	h	n	h	y	t	q	k	s	l	s	l	s	l	g	k																																		

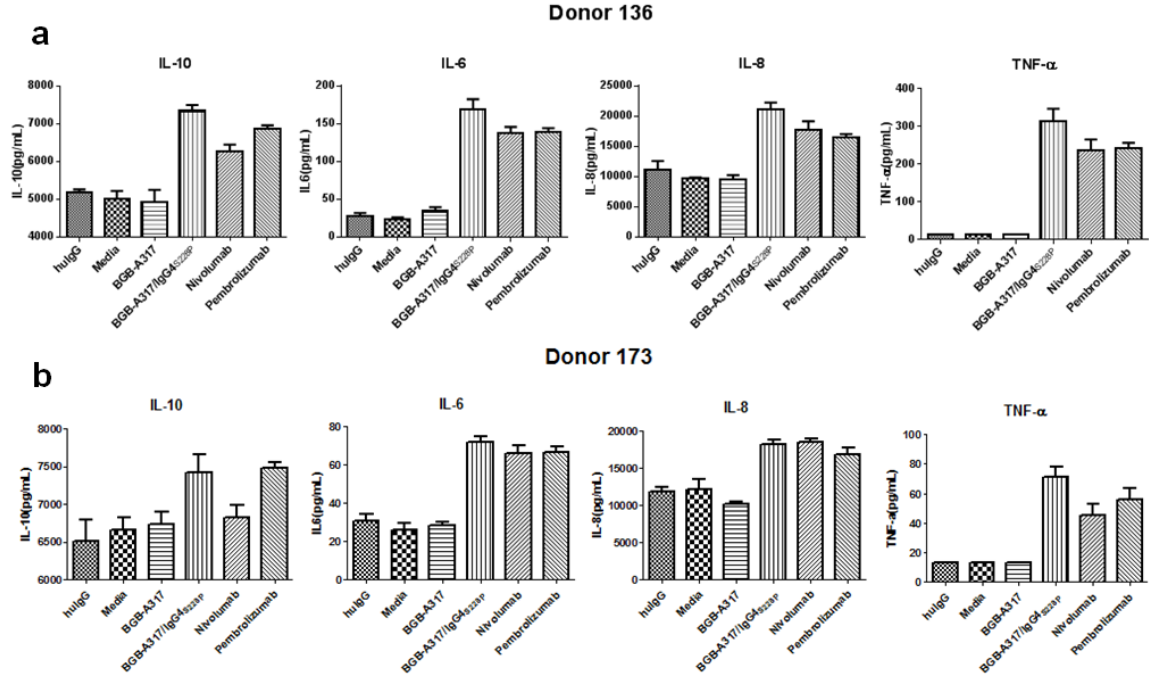
Amino acid sequence alignment of the Fc-hinge regions of IgG4_{S228P}, IgG4wt and BGB-A317 (or BGB-A317/IgG4variant). Differences in the sequences are highlighted in blue.

Supplementary figure 2



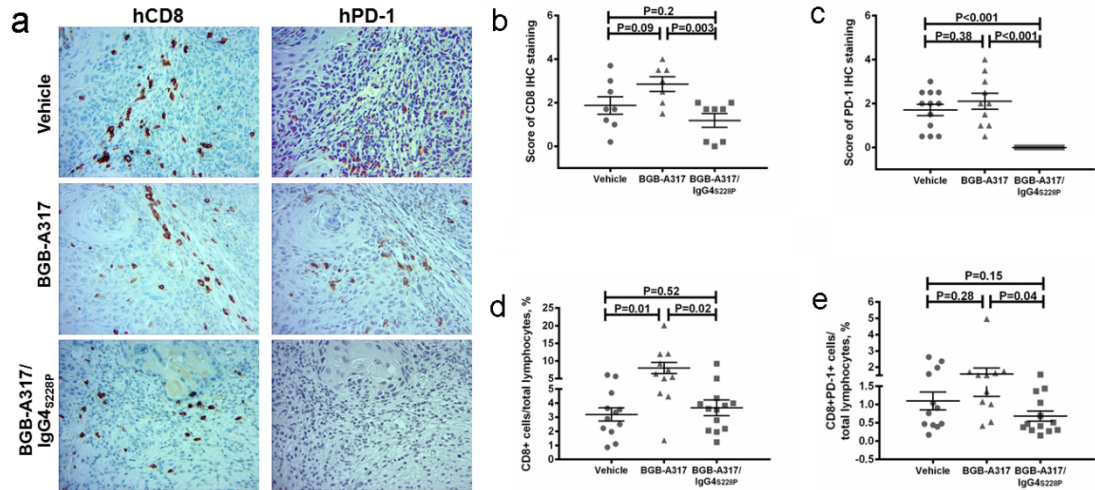
Characterization of human and mouse CD64⁺ cells within A431 allogeneic xenograft model. (a) Representative images of mCD64 and hCD64 IHC staining. (b) Comparison of mCD64⁺ and hCD64⁺ cells within tumor tissues by FACS. (Note: CD64 = FcγRIα)

Supplementary figure 3



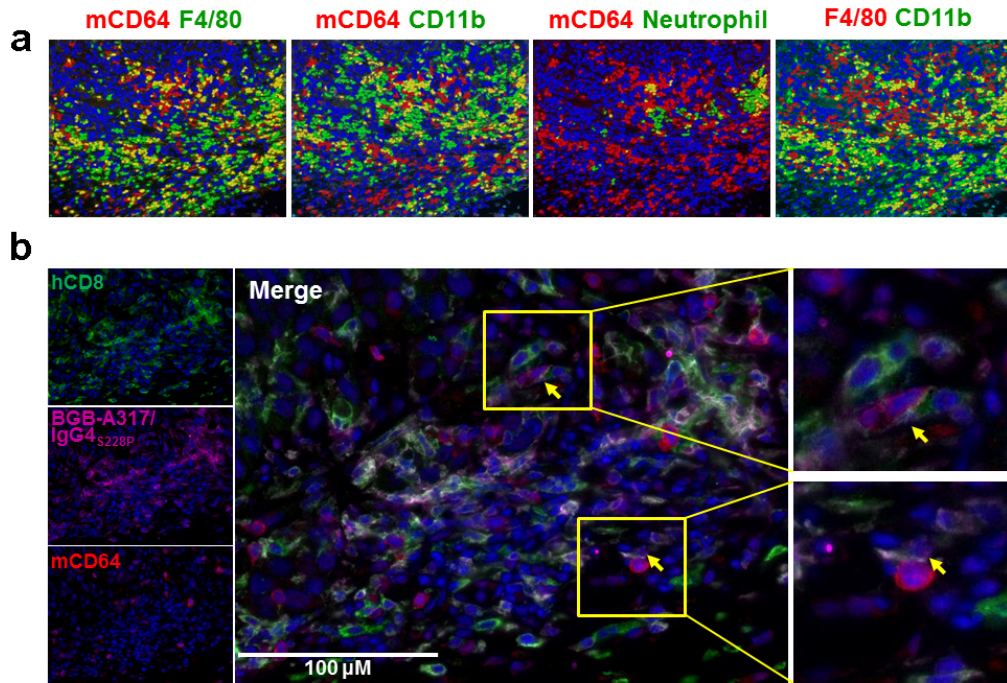
Cytokine production by M2 macrophages. To determine whether anti-PD-1 antibodies with FcγR-binding ability could activate primary M2 macrophages to increase cytokine production in response to the cross-linking with PD-1-positive HuT78/PD-1 cells, the in vitro-differentiated M2 cells (as described in the Methods and Materials) were co-cultured with HuT78/PD-1 cells in the presence of anti-PD-1 Abs at the final concentration of 10 μg/ml in 96-well v-bottomed plates. After overnight co-culture, cell-free supernatants were assayed for cytokines using a multiplex kit (Millipore, HCYTOMAG-60K) and Luminex 200 (Merck). The results of triplicate data points with M2 macrophages from two individuals (donor 136, **a** and donor 173, **b**) were presented as mean + SD (error bar).

Supplementary figure 4



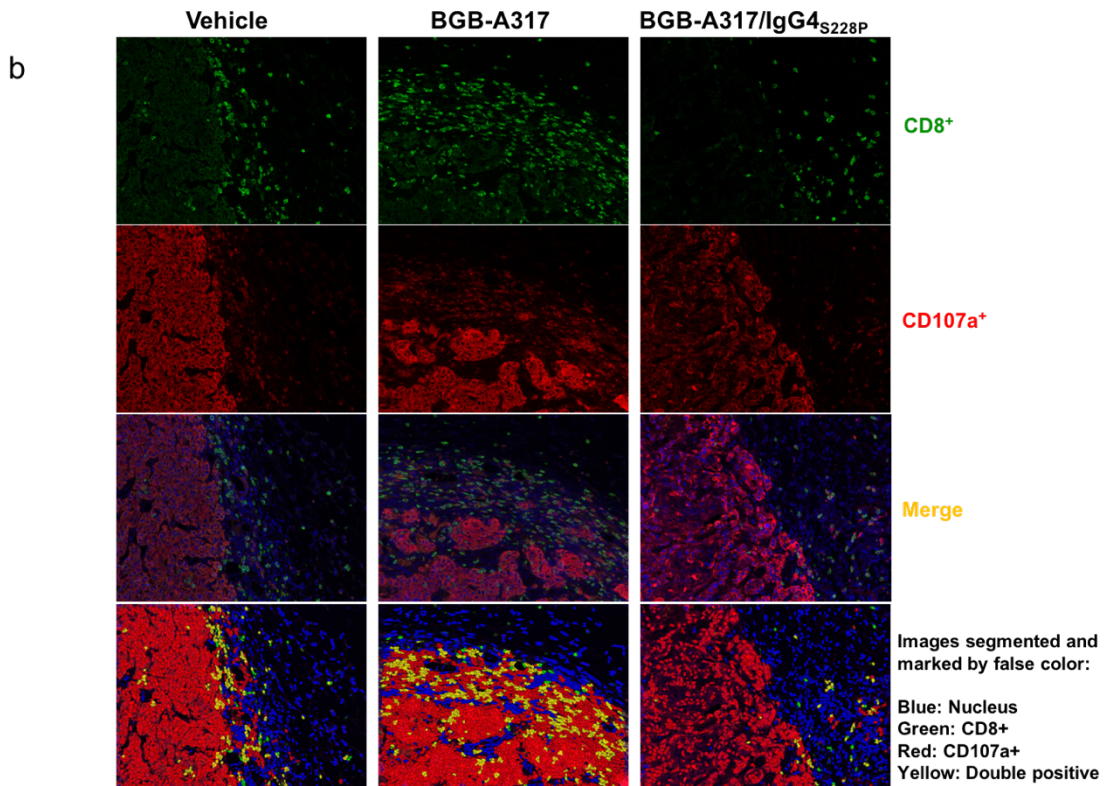
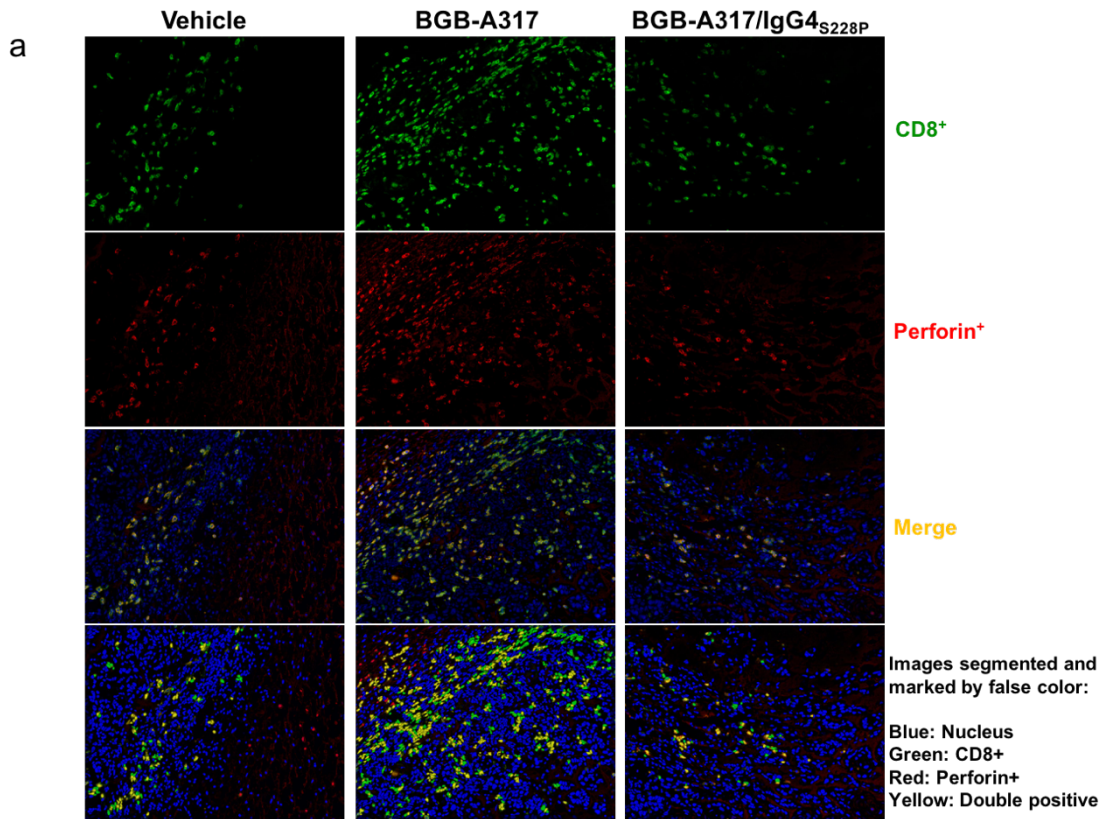
The effect of anti-PD-1 antibody treatment on tumor-infiltrating T cells. (a) Representative images of hCD8 and hPD-1 IHC staining on tumor tissues from BGB-A317- or BGB-A317/IgG4_{s228P} treated mice. (b-c) Quantified result of hCD8 and hPD-1 IHC staining intensity in indicated groups. The IHC staining intensity was scored by 2 pathologists independently. (d-e) The result of FACS analysis of tumor infiltrated hCD8 and hPD-1 positive cells in indicated groups.

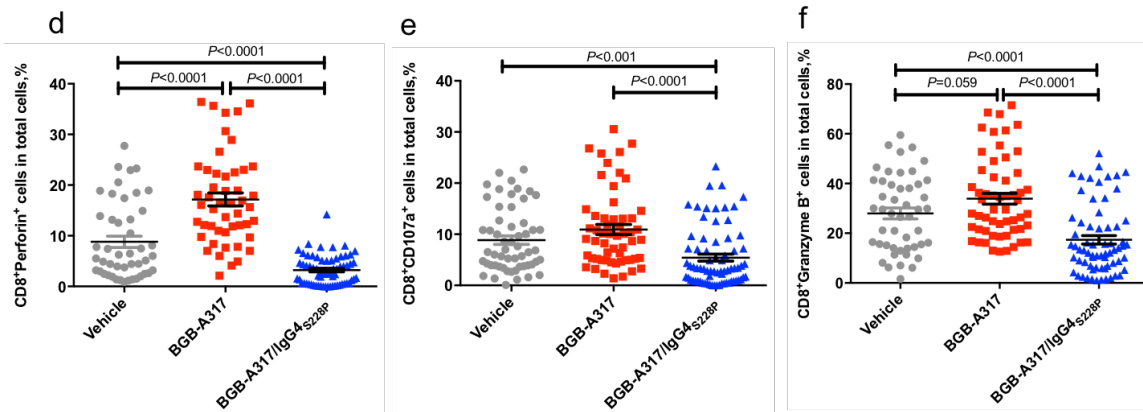
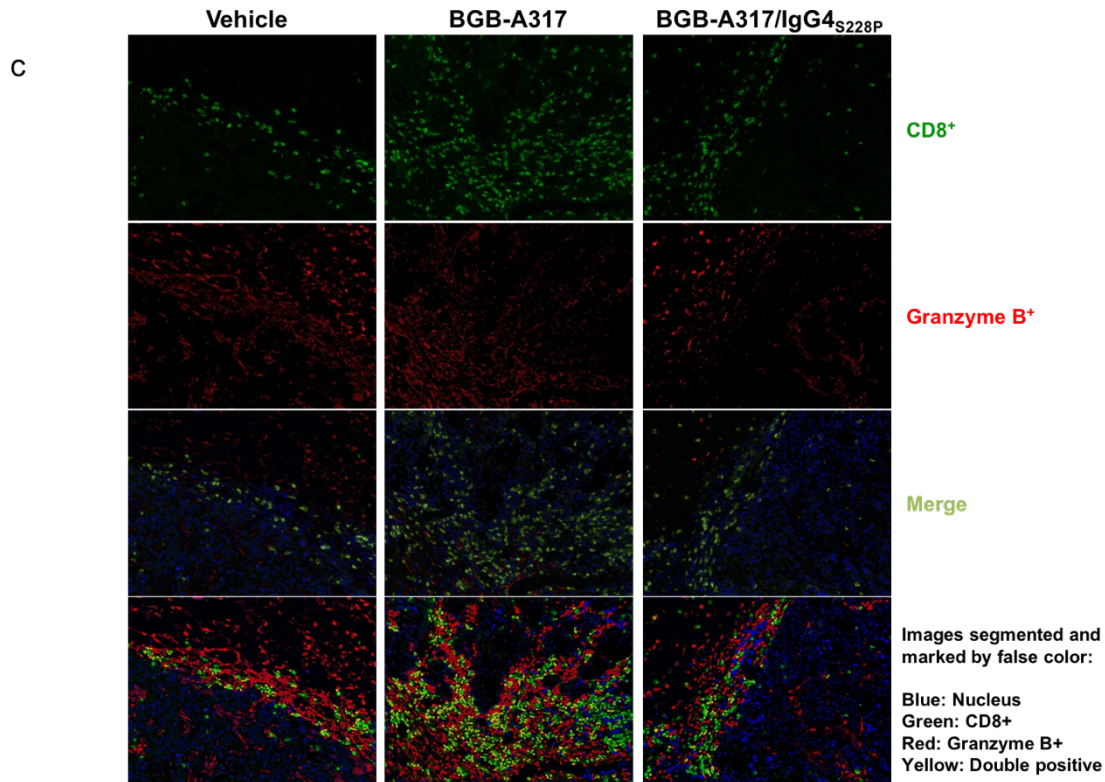
Supplementary figure 5



Multiplex immunofluorescence analysis of immune biomarkers in A431 tumor samples. (a) Digitized images of immunofluorescent staining of BGB-A317/IgG4_{S228P}-treated tumors. The same tumor section sample was stained with anti-mCD64, anti-F4/80, anti-murine CD11b, and neutrophil antibodies. Blue color presents staining of nuclei. Other immune cell biomarkers are coded by colored words on the top of the images. The immune staining photos were analyzed by inForm, and double positive cells are indicated in yellow. (b) Co-localization of BGB-A317/IgG4_{S228P} with CD8⁺ T cells and mCD64⁺ immune cells. Arrows indicate the pockets of cells co-stained positively at the junction sites by the three biomarkers: hCD8, BGB-A317/IgG4_{S228P} and mCD64. BGB-A317/IgG4_{S228P} was biotinylated and dosed at 10 mg/kg to NOD/SCID mice co-transplanted with A431 cells and human PBMCs twice a week for 3 weeks. One day after the last dose, the mice were sacrificed and the tumor tissues were processed for immunofluorescence staining by anti-hCD8, anti-mCD64 and streptavidin Alexa Fluor® 647 conjugate (Life Technologies). The images were captured by Vectra. (Note: CD64 = FcγRIα)

Supplementary figure 6





Immunofluorescence analysis of cytotoxic T cell (CTL) markers in A431 tumor samples. The tumor tissue samples of A431 xenograft mice treated with BGB-317 or BGB-A317/IgG4S228P were stained with antibodies against perforin (ab180773, Abcam), CD107a (Lysosomal-associated membrane protein 1, LAMP1, 11215-H08H, Sinobiological), or granzyme B (10345-H08H, Sinobiological) in together with CD8 (SP57, Ventana), respectively. (a-c) The representative images of the colocalization of perforin, CD107a or granzyme B with CD8⁺ T cells. The immune cell biomarkers are

color-coded by the words on the right of the images. Blue color presents staining of nuclei. The staining of perforin and granzyme B was only observed on non-tumor cells, while CD107a was also detected on tumor cells. **(d-f)** Quantification of the percentage of perforin⁺/CD8⁺, CD107a⁺/CD8⁺ and granzyme B⁺/CD8⁺ T cells within total cells in tumor samples treated with BGB-A317 or BGB-A317/IgG4S228P. The horizontal bars and P values indicates the statistical significances between the treatment groups. The images were captured by Vectra and analyzed by inForm.